

Reprinted from:

THE JOURNAL OF CHEMICAL PHYSICS

VOLUME 54, NUMBER 12

15 JUNE 1971

Coexistence Curves of CO_2 , N_2O , and CClF_3 in the Critical Region

J. M. H. LEVELT SENGERS

Heat Division, National Bureau of Standards, Washington, D. C. 20234

AND

J. STRAUB

Institut für Thermodynamik, Technische Universität, München, Germany

AND

M. VICENTINI-MISSONI

Istituto di Fisica, Università di Roma, Roma, Italy

(Received 20 November 1970)

The coexistence curves of CO_2 , N_2O , and CClF_3 are analyzed in the critical region. The curves were obtained by refractive index measurements which are virtually free of gravity effects and contain much detail near T_c . After proper weight assignment, it is established that the top of the coexistence curve is asymptotically symmetric: $\rho^\pm = \rho_c \pm B t^\beta$; that the exponent β is independent of the range, varies little from substance to substance, and is insensitive to impurities; and that the data are in agreement with the law of the rectilinear diameter. "Best" values for β , B , and for the slope of the diameter are presented. An analysis of earlier coexistence curves for CO_2 and N_2O , including a weight assignment, is presented; there is agreement between the older and newer data.

I. INTRODUCTION

A lively exchange of views on the shape of the top of the coexistence curve of gases took place around the turn of the century. Van der Waals¹ first stated that for his equation of state the top is parabolic, but later, that it was of the fourth degree. Van Laar² then showed that, as a consequence of the fact that van der Waals' equation possesses a Taylor expansion in density and temperature at the critical point, the top must be parabolic. The critical point is defined by $(\partial P / \partial \rho)_T = 0$, $(\partial^2 P / \partial \rho^2)_T = 0$, while higher density derivatives and also $\partial^2 P / \partial \rho \partial T$ are nonzero. Van Laar proceeded by postulating that the liquid and gas densities along the coexistence curve, ρ^+ and ρ^- , respectively, can be written in terms of powers of the reduced temperature $t = (T - T_c) / T_c$ as follows:

$$\rho^\pm = \rho_c (1 + B_1 t^\beta + B_2 t^{2\beta} + \dots). \quad (1)$$

By applying the Maxwell construction to the Taylor

expansion of the van der Waals equation, van Laar deduced values for the exponent β and the coefficients B^\pm . Thus, he found that $\beta = \frac{1}{2}$ and established the symmetry character of the terms in the expansion: $B_1^+ = -B_1^-$, $B_2^+ = B_2^-$, etc. He also noted that these findings, depending only on the existence of a Taylor expansion, did not depend on the particular form of the van der Waals equation. Consequently, all equations analytic at the critical point and for which $(\partial P / \partial \rho)_T$, $(\partial^2 P / \partial \rho^2)_T$ are zero but $(\partial^3 P / \partial \rho^3)_T$, $\partial^2 P / \partial \rho \partial T$ nonzero, will have coexistence curves of the following form:

$$\rho^\pm = \rho_c (1 \pm B_1 |t|^{1/2} + B_2 |t| \pm B_3 |t|^{3/2} + \dots), \quad (2)$$

where the plus again refers to the liquid and the minus to the gas density. Thus

$$(\rho_L - \rho_G) / 2\rho_c = B_1 |t|^{1/2} + B_3 |t|^{3/2} + \dots, \quad (3)$$

$$(\rho_L + \rho_G) / 2\rho_c = B_2 |t| + B_4 |t|^2 + \dots. \quad (4)$$

Equation (4) expresses the well-known law of the

rectilinear diameter whereas (3) states that the top of the coexistence curve is a parabola.

Van Laar² also noted that if not two but four derivatives of pressure with respect to density were put equal to zero at the critical point, β would be $1/4$. This special case has later been studied by Planck³ and Baehr.⁴ Baehr calculated a number of coefficients in the expansion (1) with $\beta = \frac{1}{4}$. For this case, the diameter is obviously not straight but it is a parabola asymptotically.

It is well known that the classical predictions, $\beta = \frac{1}{2}$ or $\frac{1}{4}$, are in conflict with experiment. Verschaffelt,⁵ around 1900, found that the coexistence curves of CO_2 and H_2 have β approximately $1/3$. An extensive paper by Goldhammer,⁶ in 1910, presents reasonable descriptions of coexistence curves of 12 substances using $\beta = \frac{1}{3}$, much to the distress of van Laar.² This experimental fact cannot be taken lightly. It is inconsistent with classical theory. Either, as van Laar tried to argue, the cubic character found by Verschaffelt and Goldhammer breaks down when the critical point is approached, or, contrary to classical theory, a Taylor expansion of the equation of state of real fluids does not exist at the critical point. From the wealth of data accumulated on coexistence curves, no clear evidence for a change of power law behavior when the critical point is approached has been found and the analysis presented here is no exception. However, the second option, nonanalyticity at the critical point, has become generally accepted only in the last decade.⁷ Once this possibility is admitted, however, the nice symmetry features of the classical case are lost and we might, in general, have a coexistence curve equation as bad looking as

$$\rho^\pm = \rho_c [1 + B_1^\pm |t|^{\beta_1^\pm} + B_2^\pm |t|^{\beta_2^\pm} + \dots], \quad (5)$$

where

$$\beta_1^+ < \beta_2^+ < \dots, \quad \beta_1^- < \beta_2^- < \dots.$$

Theoretical models for nonanalytic critical points, such as the lattice gas version of the Ising model, are not very suggestive in the study of the coexistence curves of gases since they have a built-in symmetry, $\rho^+ + \rho^- = 2\rho_c$, which is absent in real gases. One of the purposes of this paper will be to demonstrate that, in spite of the nonanalyticity, certain symmetry features established by van Laar for the classical case seem to be present in real gases as well, namely $B_1^+ = -B_1^-$, $\beta_1^+ = \beta_1^-$, and very likely $B_2^+ \cong B_2^-$, $\beta_2^+ = \beta_2^-$.

These conclusions could be reached only after a careful error assessment and weighing procedure had been established for several sets of precise coexistence curve data obtained by refractive index measurements. Also a detailed study of ranges of asymptotic validity of the terms in (5) was made. The symmetry character of (5) results in a simple procedure for determining best values of B_1 , β_1 , and B_2 for the substances studied. The values are reported, and some comments on their

universality are made. The effect of impurities on the value of β_1 will be shown to be minimal. The results of the optical experiments will be compared with some coexistence curves obtained by more classical methods and these two sets of results will be found to agree.

II. THE EXPERIMENTAL DATA

The coexistence curves we have analyzed are those of CO_2 , N_2O (pure and impure), and CClF_3 . The most extensive body of data on those substances was obtained by Schmidt and Straub⁸ at the Technische Universität in München. For comparison, we have also analyzed coexistence curve data on CO_2 obtained by Michels and co-workers,⁹ and data on N_2O measured by Cook.¹⁰

The experimental method used by the München group is the determination of the refractive index of the two coexisting phases. The method has been discussed elsewhere⁸; briefly, a narrow beam of parallel sodium light is passed through a sample of gas enclosed in a carefully thermostated pressure vessel with two parallel windows. A prism is immersed in the fluid, the deflection of the light being a measure of the refractive index of the fluid. Density gradients present in the fluid near the critical point because of gravity result in height dependence of the angle of deflection of the beam. If there are two phases present, a sharp shift in the angle of deflection occurs at the interface, enabling a precise determination of both indices of refraction right at the interface; thus, the fact that density gradients are induced by gravity in the bulk of each phase in near-critical states is not a source of error in this experiment, in contrast with most other determinations of orthobaric densities.

The refractive index data obtained by this method for CO_2 , N_2O (pure and impure), and CClF_3 are summarized in Table I. The temperatures are on the I.P.T.S. '48 as recorded in the experiment.

The coexisting densities of CO_2 determined by Michels⁹ were obtained in the course of *PVT* determinations as intercepts of isotherms with vapor pressure; the coexisting densities of N_2O measured by Cook¹⁰ were obtained by varying the volume of a known amount of fluid until the other phase began to form. These sets of data will be summarized later in Secs. IX and X, respectively. Cook recorded his temperatures on I.P.T.S. '27 or '48; there is uncertainty about the scale used by Michels.

III. METHOD OF ANALYSIS

The measured refractive indices can be related to densities using the Lorentz-Lorenz relation

$$(n^2 - 1)/(n^2 + 2) = (4\pi\alpha/3)\rho. \quad (6a)$$

Here n is the refractive index, α the polarizability of a molecule, and ρ the density $\rho = N/V$. The Lorentz-Lorenz equation is a generalization to nonzero electric field frequency of the Clausius-Mosotti equation

$$(\epsilon - 1)/(\epsilon + 2) = (4\pi\alpha/3)\rho. \quad (6b)$$

TABLE I. Experimental refractive index data.

T (°C)	n_L	n_G	T (°C)	n_L	n_G
CO ₂ Series I $T_c(\text{obs}) = 31.030^\circ\text{C}$ $n_c(\text{obs}) = 1.1062$			N ₂ O pure $T_c(\text{obs}) = 36.416^\circ\text{C}$ $n_c(\text{obs}) = 1.1154$		
31.027	1.11066	1.10240	36.415	1.1195	1.1111
31.026	1.11135	1.10213	36.411	1.1203	1.1105
31.024	1.11172	1.10155	36.410	1.1211	1.1102
31.023	1.11210	1.10136	36.408	1.1216	1.1096
31.021	1.11230	1.10080	36.367	1.1264	1.1048
31.019	1.111280	1.10015	36.291	1.1308	1.1005
[30.974	1.1181	1.0952]	36.127	1.1359	1.0956
30.465	1.130834	1.082781	36.013	1.1385	1.0932
[29.792	1.138496	1.075885]	34.900	1.1518	1.0807
28.430	1.148333	1.066719	32.540	1.1667	1.0679
25.687	1.161106	1.056453	30.426	1.1758	1.0606
22.752	1.170953	1.049101	28.464	1.1827	1.0552
CO ₂ Series II $T_c(\text{obs}) = 30.991^\circ\text{C}$			26.130	1.1897	1.0501
30.989	1.11087	1.10451	25.315	1.1918	1.0485
30.988	1.11158	1.10405	24.125	1.1949	1.0464
30.987	1.11200	1.10334	23.835	1.1956	1.0461
30.984	1.11355	1.10271	N ₂ O with 1.1% H ₂ O		
30.982	1.11371	1.10207	36.101	1.1374	1.0934
30.978	1.11463	1.10109	35.170	1.1499	1.0821
30.970	1.11576	1.10006	34.198	1.1573	1.0754
30.958	1.11733	1.09864	32.274	1.1677	1.0663
30.950	1.11787	1.09810	30.387	1.1756	1.0601
30.926	1.11949	1.09669	28.459	1.1823	1.0551
30.884	1.12165	1.09429	26.510	1.1880	1.0506
30.833	1.12381	1.09218	24.583	1.1932	1.0469
30.706	1.12728	1.08886	22.737	1.1197	1.0433
30.662	1.1283	1.08791	N ₂ O with 0.39 mole% air		
30.541	1.13059	1.08578	35.728	1.1382	1.0927
30.312	1.13410	1.08248	34.978	1.1479	1.0833
29.734	1.14047	1.07654	33.962	1.1562	1.0760
29.115	1.14556	1.07195	32.021	1.1672	1.0668
28.597	1.14904	1.06895	29.528	1.1775	1.0586
27.828	1.15343	1.06517	25.836	1.1889	1.0499
26.683	1.15898	1.06049	23.280	1.1955	1.0453
25.480	1.16398	1.05646			
23.543	1.17076	1.05127			
21.508	1.17681	1.04674			
CClF ₃ $T_c(\text{obs}) = 28.715^\circ\text{C}$ $n_c(\text{obs}) = 1.0996$					
28.685	1.1079	1.0918			
28.650	1.1105	1.0894			
28.473	1.1160	1.0839			
27.860	1.1255	1.0750			
26.770	1.1345	1.0668			
25.035	1.1439	1.0589			
21.770	1.1554	1.0496			

This generalization is justified in the absence of dispersion, i.e., in the absence of low-lying optical levels. The Clausius-Mosotti equation, on the other hand, is also approximate. It has been obtained for a system of nonpolar spherical molecules with constant polarizability α while neglecting fluctuations in the local field.¹¹ None of the conditions for the validity of (6a)

are fulfilled for the gases discussed here. The molecules of CO₂, N₂O, and CClF₃ are all nonspherical; N₂O has a small, CClF₃ an appreciable dipole moment; CO₂ has nonnegligible dispersion; moreover, density-dependent fluctuation corrections to the rhs of (6) are expected theoretically¹¹ and have been found experimentally for CO₂¹² and other gases¹³; finally, there are reasons to

believe that the molecular polarizability α itself could be density dependent as well.¹¹ The experimental evidence,^{12,13} however, suggests that at least for non-polar gases the density-dependent corrections to (6) are no more than a few percent and vary slowly, whereas temperature-dependent corrections are practically negligible. For an analysis of asymptotic behavior near the critical point the use of (6) without correction terms seems therefore justified. A more serious question is whether the quantity $(n^2-1)/(n^2+2)\rho$ might be anomalous at the critical point. As Larsen, Mountain, and Zwanzig¹⁴ pointed out, critical opalescence indicates that at least the imaginary part of the refractive index is anomalous, while the homogeneity of the medium assumed in deriving (6a) is certainly not present near the critical point. However, their estimate of the size of the anomaly in n shows that it is negligible for practical purposes, namely no more than 1×10^{-4} in n . Henceforth we will consider the quantity $LL = (n^2-1)/(n^2+2)$ as being proportional to the density. A check on this assumption is made by comparing with coexistence curve data obtained by more traditional methods. The agreement is good (Secs. IX, X).

The data analysis, after weights are properly assigned (Sec. IV), will go in four steps. First, the quantities $LL_L - LL_C$, $LL_C - LL_G$ are fitted separately to temperature functions of the form $B_1 |t|^{\beta_1}$. It is shown that $B_1^+ = -B_1^-$, $\beta_1^+ = \beta_1^-$, asymptotically, when the range is reduced. Next, it is shown that the diameter $LL_L + LL_G$ is straight within error. Then, it is shown that the next term in (5) has roughly the same coefficient on the two sides. Thus, in taking the difference $LL_L - LL_G$, this term cancels and a large asymptotic range for the leading term $B_1 |t|^{\beta_1}$ in (5) is obtained. Best values for B_1 , β_1 are obtained by a least-squares analysis of the difference $LL_L - LL_G$.

IV. THE ASSIGNMENT OF ABSOLUTE WEIGHTS

In the analysis we propose to carry out proper weight assignment is imperative. In the München experiments the distance to the critical temperature varies from 10°C to a few millidegrees; temperature errors propagated into the LL values greatly diminish their accuracy near T_c . In the weight assignment we have assumed that there are two independent sources of error: namely those in the refractive index and those in the temperature measurement characterized by standard deviations σ_n and σ_T , respectively. The standard deviation of the LL values is then calculated using propagation of error.

By differentiating (6) and substituting approximate values $n_L \sim 1.1$, $n_G \sim 1.05$ we find for the standard deviation of LL the value $0.58n\sigma_n$ due to errors in measurement of n . Thus

$$\text{Var}_n\{LL\} = (0.58n\sigma_n)^2, \quad (7a)$$

$$\begin{aligned} \text{Var}_n\{LL_L - LL_G\} &= \text{Var}_n\{LL_L + LL_G\} \\ &= (0.58)^2(n_L^2 + n_G^2)\sigma_n^2, \end{aligned} \quad (7b)$$

where the subscript n denotes contributions to the variance of the quantity in braces due to errors in n .

However, a temperature measurement with s.d. σ_T is made simultaneously. Since LL_L , LL_G vary with temperature roughly as $B_1 |t|^{\beta_1}$, (5), we have, due to temperature errors alone,

$$\begin{aligned} \sigma_T\{LL_L\} &= \sigma_T\{LL_G\} = B_1\beta_1 |t|^{\beta_1-1}\sigma_t \\ &= \frac{1}{2}(LL_L - LL_G)(\beta_1\sigma_t/|t|). \end{aligned} \quad (8)$$

Thus, from (7) and (8)

$$\begin{aligned} \text{Var}\{LL\} &= \text{Var}_n\{LL\} + \text{Var}_T\{LL\} \\ &= (0.58n\sigma_n)^2 + \frac{1}{4}(LL_L - LL_G)^2(\beta_1^2\sigma_t^2/t^2). \end{aligned} \quad (9)$$

However, since the two refractive indices n_L , n_G are measured almost simultaneously there is a correlation between the variations in LL_L and LL_G caused by temperature error: there is partial cancellation when the sum $LL_L + LL_G$ is formed, but not when the difference is formed. We have roughly taken this effect into account by assuming $\text{Var}_T\{LL_L + LL_G\}$ to be one-half that of $\text{Var}_T\{LL_L - LL_G\}$.

Summarizing, we have weighted sums and differences according to the following variances:

$$\begin{aligned} \text{Var}\{LL_L + LL_G\} &= (0.58)^2(n_L^2 + n_G^2)\sigma_n^2 + \frac{1}{4}(LL_L - LL_G)^2(\beta_1^2\sigma_t^2/t^2), \\ \text{Var}\left\{\frac{LL_L - LL_G}{LL_C}\right\} &= \frac{[(0.58)^2(n_L^2 + n_G^2)\sigma_n^2 + \frac{1}{2}(LL_L - LL_G)^2(\beta_1^2\sigma_t^2/t^2)]}{LL_C^2}. \end{aligned} \quad (10)$$

What we refer to as the estimated errors of the experimental values are the square roots of the variances (9) or (10). The weights used in the fits are the inverses of the variances (9) and (10). We have used $\sigma_n = 1 \times 10^{-4}$ and $\sigma_T = 0.001^\circ\text{C}$. It is stressed that if absolute weights are properly assigned, the standard deviation of the proper model function should be near unity and the experimental points should rarely deviate more than two times their estimated error.

The least-squares fitting routine used throughout is that of Ref. 15.

V. THE LEADING TERM $B_1 \pm |t|^{\beta_1 \pm}$

We have studied the behavior of $LL - LL_C = B_1 \pm |t|^{\beta_1 \pm}$ as a function of the temperature range from critical. The München data will be shown to permit only minor variations in the value of T_c (Sec. VII); therefore, we have only used the optimum value here. The data for CO_2 series II and for N_2O are sufficiently plentiful to permit an analysis. In Tables II and III, we show as functions of $|t|_{\text{max}}$, values of $\ln |B_1^+|$, β_1^+ , $\ln |B_1^-|$, β_1^- , their standard deviations and the standard deviation of the fit; this is done for three

TABLE II. Asymptotic range of $LL-LL_C$: CO_2 Series II.

$ t _{\max}$ (%)	LL_C	Liquid $(LL_L-LL_C)/LL_C$					Gas $(LL_G-LL_C)/LL_C$				
		s.d.	$\ln B_1^+$	s.d.	β_1^+	s.d.	s.d.	$\ln B_1^-$	s.d.	β_1^-	s.d.
3.12	0.7058	2.25	0.7469 ± 0.0066		0.3596 ± 0.0014		1.19	0.5898 ± 0.0034		0.3349 ± 0.0007	
	0.7048	2.44	0.7433 ± 0.0071		0.3576 ± 0.0015		1.30	0.5955 ± 0.0037		0.3367 ± 0.0008	
	0.7038	2.65	0.7397 ± 0.0076		0.3557 ± 0.0017		1.44	0.6012 ± 0.0041		0.3386 ± 0.0009	
1.81	0.7058	1.51	0.7239 ± 0.0062		0.3556 ± 0.0012		0.82	0.6010 ± 0.0032		0.3368 ± 0.0006	
	0.7048	1.66	0.7186 ± 0.0068		0.3534 ± 0.0013		0.85	0.6084 ± 0.0034		0.3390 ± 0.0007	
	0.7038	1.82	0.7135 ± 0.0074		0.3512 ± 0.0014		0.92	0.6159 ± 0.0037		0.3411 ± 0.0007	
1.04	0.7058	0.98	0.7024 ± 0.0057		0.3522 ± 0.0010		0.85	0.6024 ± 0.0048		0.3371 ± 0.0008	
	0.7048	1.08	0.6953 ± 0.0062		0.3497 ± 0.0011		0.87	0.6118 ± 0.0049		0.3395 ± 0.0009	
	0.7038	1.19	0.6882 ± 0.0068		0.3472 ± 0.0012		0.92	0.6213 ± 0.0052		0.3419 ± 0.0009	
0.62	0.7058	0.82	0.6869 ± 0.0071		0.3500 ± 0.0011		0.90	0.6047 ± 0.0074		0.3374 ± 0.0012	
	0.7048	0.87	0.6772 ± 0.0074		0.3471 ± 0.0012		0.90	0.6166 ± 0.0075		0.3402 ± 0.0012	
	0.7038	0.94	0.6677 ± 0.0079		0.3443 ± 0.0013		0.92	0.6287 ± 0.0077		0.3430 ± 0.0012	
0.22	0.7058	0.75	0.6673 ± 0.0122		0.3473 ± 0.0017		0.94	0.5962 ± 0.0146		0.3362 ± 0.0021	
	0.7048	0.73	0.6515 ± 0.0117		0.3436 ± 0.0017		0.95	0.6143 ± 0.0151		0.3399 ± 0.0021	
	0.7038	0.72	0.6360 ± 0.0115		0.3400 ± 0.0016		0.98	0.6328 ± 0.0157		0.3436 ± 0.0022	
0.11	0.7058	0.81	0.6725 ± 0.0202		0.3479 ± 0.0027		0.97	0.6149 ± 0.0232		0.3385 ± 0.0031	
	0.7048	0.79	0.6515 ± 0.0194		0.3436 ± 0.0026		0.96	0.6384 ± 0.0233		0.3429 ± 0.0031	
	0.7038	0.77	0.6312 ± 0.0187		0.3393 ± 0.0025		0.95	0.6625 ± 0.0235		0.3473 ± 0.0031	

TABLE III. Asymptotic range of $LL-LL_C$: N_2O .

$ t _{\max}$ (%)	t_{\max} (%)	LL_C	Liquid $(LL_L-LL_C)/LL_C$					Gas $(LL_G-LL_C)/LL_C$				
			s.d.	$\ln B_1^+$	s.d.	β_1^+	s.d.	s.d.	$\ln B_1^-$	s.d.	β_1^-	s.d.
4.1		0.7544	2.67	0.7442 ± 0.0070		0.3632 ± 0.0018		2.11	0.5531 ± 0.0053		0.3325 ± 0.0014	
		0.7534	2.83	0.7421 ± 0.0074		0.3616 ± 0.0019		2.26	0.5571 ± 0.0057		0.3340 ± 0.0015	
		0.7524	3.01	0.7401 ± 0.0078		0.3600 ± 0.0020		2.42	0.5617 ± 0.0062		0.3354 ± 0.0016	
3.6		0.7544	2.55	0.7369 ± 0.0078		0.3618 ± 0.0019		1.46	0.5618 ± 0.0043		0.3342 ± 0.0011	
		0.7534	2.70	0.7344 ± 0.0082		0.3601 ± 0.0020		1.63	0.5663 ± 0.0048		0.3358 ± 0.0012	
		0.7524	2.87	0.7319 ± 0.0086		0.3584 ± 0.0021		1.81	0.5708 ± 0.0054		0.3373 ± 0.0013	
2.6		0.7544	2.04	0.7206 ± 0.0083		0.3588 ± 0.0018		1.04	0.5718 ± 0.0041		0.3360 ± 0.0009	
		0.7534	2.16	0.7172 ± 0.0087		0.3569 ± 0.0019		1.20	0.5773 ± 0.0047		0.3378 ± 0.0010	
		0.7524	2.29	0.7138 ± 0.0092		0.3551 ± 0.0020		1.37	0.5828 ± 0.0054		0.3395 ± 0.0012	
1.94		0.7544	1.64	0.7081 ± 0.0083		0.3567 ± 0.0017		1.04	0.5748 ± 0.0050		0.3365 ± 0.0010	
		0.7534	1.72	0.7040 ± 0.0086		0.3547 ± 0.0018		1.19	0.5810 ± 0.0058		0.3384 ± 0.0012	
		0.7524	1.82	0.6999 ± 0.0091		0.3527 ± 0.0019		1.35	0.5872 ± 0.0066		0.3403 ± 0.0014	
1.25		0.7544	1.27	0.6919 ± 0.0088		0.3541 ± 0.0016		0.96	0.5817 ± 0.0064		0.3376 ± 0.0012	
		0.7534	1.29	0.6865 ± 0.0089		0.3520 ± 0.0016		1.09	0.5892 ± 0.0073		0.3397 ± 0.0014	
		0.7524	1.33	0.6812 ± 0.0091		0.3498 ± 0.0017		1.23	0.5968 ± 0.0084		0.3418 ± 0.0015	
0.49		0.7544	1.05	0.6671 ± 0.0135		0.3505 ± 0.0021		0.94	0.5934 ± 0.0115		0.3393 ± 0.0018	
		0.7534	0.95	0.6582 ± 0.0121		0.3478 ± 0.0019		1.02	0.6045 ± 0.0127		0.3420 ± 0.0020	
		0.7524	0.87	0.6494 ± 0.0109		0.3451 ± 0.0017		1.13	0.6158 ± 0.0142		0.3446 ± 0.0023	
0.13		0.7544	0.80	0.7213 ± 0.0246		0.3578 ± 0.0034		0.83	0.6309 ± 0.0244		0.3444 ± 0.0034	
		0.7534	0.79	0.7017 ± 0.0238		0.3537 ± 0.0033		0.84	0.6523 ± 0.0251		0.3484 ± 0.0035	
		0.7524	0.79	0.6826 ± 0.0234		0.3496 ± 0.0033		0.86	0.6741 ± 0.0262		0.3525 ± 0.0037	

choices of LL_C , the center one being the optimum (Sec. VII). For the larger values of $|t|_{\max}$, there are sizeable systematic differences in exponents and coefficients on gas and liquid side. Also, the standard deviation of the fit decreases when $|t|_{\max}$ goes from several percent to 1%. For ranges smaller than 0.3% the coefficients $|B_1^+|$, $|B_1^-|$ and the exponents β_1^+ , β_1^- become equal within error for gas and liquid. For the exponent, the approach to equal values with shrinking temperature range is shown for CO_2 in Fig. 1 and for N_2O in Fig. 2.

VI. THE DIAMETER

The exponent β_2^+ in (5) is not necessarily equal to β_2^- . In view of the limited temperature range of the experimental data, it has proven impossible to ascertain whether β_2^+ equals β_2^- or not. However, starting from the likely premise that the exponents *are* equal on the

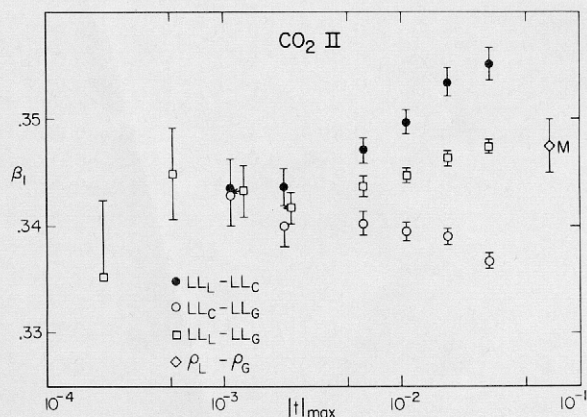


FIG. 1. The apparent values of β_1^\pm of CO_2 in $LL-LL_C = B_1|t|^{\beta_1}$ as functions of the reduced temperature range $|t|_{\max}$. Error bars denote ± 1 s.d. For $|t|_{\max} < 3 \times 10^{-3}$ the exponents for gas and liquid side become equal within error. The point marked *M* represents the β value derived for Michels' CO_2 data.

two sides, and using the fact that the leading term is symmetric, it follows immediately from (5) that

$$\frac{1}{2}(LL_L + LL_G) = LL_C \left\{ 1 + \frac{1}{2}(B_2^+ + B_2^-) |t|^{\beta_2} \dots \right\}. \quad (11)$$

As was discussed in the Introduction, for classical equations of the van der Waals type $\beta_2 = 2\beta_1 = 1$ corresponds to the law of the rectilinear diameter (the special classical case with $\beta_1 = \frac{1}{4}$ has a curved diameter). There is no *a priori* reason why the law of the rectilinear diameter should hold for a nonclassical critical point. We have carefully investigated the optical data with this point in mind. The data for $LL_L + LL_G$ are listed in Tables IV–VII. We will demonstrate that a straight line fits these data within errors. If a curved diameter of the form $|t|^{1-\alpha}$ is admitted, as was recently found in model calculations¹⁶ and also on thermodynamic grounds,¹⁷ the present data, if anything, seem to favor slightly negative values of α , contrary to the

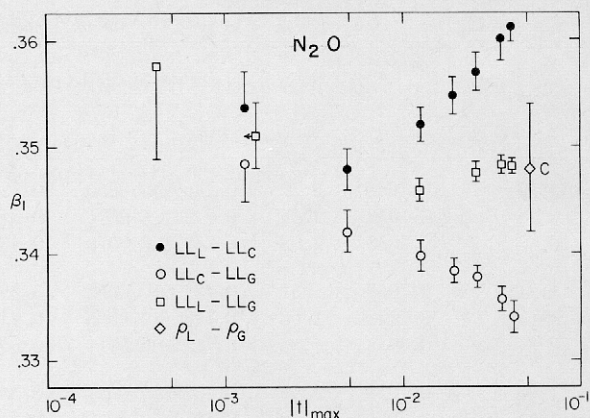


FIG. 2. As Fig. 1, but for N_2O . The point marked *C* represents the β value derived from Cook's N_2O data.

general finding that α is slightly positive and perhaps as large as $1/8$.

A. CO_2 Series I

The difference between experimental and calculated values of $LL_L + LL_G$ when fitting with a straight line and using $T_c = 31.030^\circ\text{C}$ is shown in Fig. 3. There is a slight evidence of systematic behavior, barely outside the experimental error. It suggests that the diameter might curve upward (α negative). This

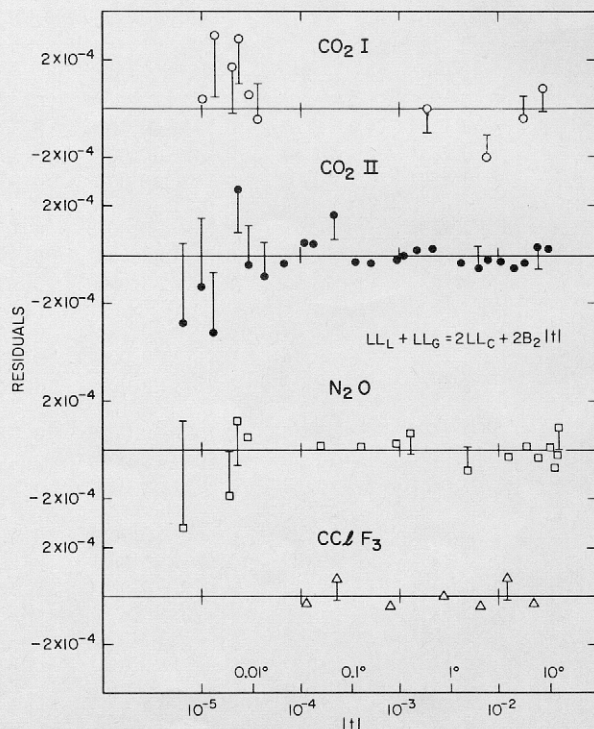


FIG. 3. Residuals of the fit of $LL_L + LL_G$ to a linear function of $|t|$ for the four sets of data. Bars denote estimated errors of the experimental data.

TABLE IV. CO₂ Series I.

Temperature (°C)	LL_L	LL_G	(LL_L+LL_G)			$(LL_L-LL_G)/LL_G$		
			Value	10 ⁵ err	10 ⁵ res	Value	10 ⁴ err	10 ⁴ res
31.027	0.07223	0.06696	0.13919	29	4	0.0758	58	34
31.026	0.07267	0.06678	0.13946	25	31	0.0846	49	46
31.024	0.07291	0.06641	0.13932	20	17	0.0933	37	12
31.023	0.07315	0.06629	0.13944	18	29	0.0986	34	14
31.021	0.07328	0.06593	0.13921	16	6	0.1056	29	-4
31.019	0.07359	0.06552	0.13911	15	-4	0.1161	27	26
30.465	0.08503	0.05435	0.13938	9	0	0.4410	13	-10
28.430	0.09602	0.04394	0.13997	9	-22	0.7486	13	3
25.687	0.10399	0.03725	0.14124	9	-4	0.9592	13	-2
22.752	0.11009	0.03245	0.14254	9	9	1.1160	13	2
$T_c=31.030$			$2LL_G=0.13915$			$\ln 2B_1=1.3528$		
			± 7			± 25		
			Slope $a=0.121$			$B_1=1.935$		
			± 5			$\beta_1=0.3450$		
			$a^*=a/2LL_G=0.87$			± 6		
			s.d.=1.22			s.d.=0.62		

TABLE V. CO₂ Series II.

Temperature (°C)	LL_L	LL_G	(LL_L+LL_G)			$(LL_L-LL_G)/LL_G$		
			Value	10 ⁶ err	10 ⁶ res	Value	10 ⁴ err	10 ⁴ res
30.989	0.07237	0.06831	0.14067	34	-29	0.0576	66	-42
30.988	0.07282	0.06801	0.14083	27	-13	0.0682	53	-31
30.987	0.07309	0.06756	0.14064	24	-32	0.0784	46	-4
30.984	0.07407	0.06716	0.14123	18	27	0.0981	34	25
30.982	0.07417	0.06675	0.14092	16	-4	0.1054	29	10
30.978	0.07476	0.06612	0.14088	14	-8	0.1226	25	40
30.970	0.07548	0.06546	0.14094	12	-3	0.1422	20	20
30.958	0.07648	0.06455	0.14103	11	5	0.1692	17	53
30.950	0.07682	0.06420	0.14102	10	5	0.1790	16	21
30.926	0.07785	0.06330	0.14115	10	16	0.2064	15	-12
30.884	0.07922	0.06176	0.14098	10	-2	0.2477	14	9
30.833	0.08059	0.06040	0.14099	9	-3	0.2864	14	37
30.706	0.08278	0.05827	0.14105	9	-2	0.3478	13	9
30.662	0.08343	0.05766	0.14108	9	-0	0.3657	13	9
30.541	0.08487	0.05628	0.14116	9	3	0.4057	13	-10
30.312	0.08709	0.05415	0.14124	9	2	0.4673	13	-19
29.734	0.09109	0.05031	0.14141	9	-3	0.5786	13	-25
29.115	0.09429	0.04734	0.14163	9	-5	0.6661	13	-17
28.597	0.09647	0.04539	0.14186	9	-1	0.7246	13	-22
27.828	0.09921	0.04294	0.14214	9	-2	0.7984	13	-23
26.683	0.10267	0.03989	0.14255	9	-5	0.8907	13	-7
25.480	0.10577	0.03726	0.14303	9	-3	0.9721	13	10
23.543	0.10997	0.03387	0.14384	9	4	1.0798	13	16
21.508	0.11371	0.03090	0.14461	9	3	1.1749	13	22
$T_c=30.991^\circ\text{C}$			$2LL_G=0.14096$			$\ln 2B_1=1.3642$		
			± 2			± 29		
			Slope $a=0.116$			$B_1=1.957$		
			± 2			$\beta_1=0.3475$		
			$a^*=a/2LL_G=0.82$			± 6		
			s.d.=0.68			s.d.=1.42		

TABLE VI. N₂O.

Temperature (°C)	LL_L	LL_G	$(LL_L + LL_G)$			$(LL_L - LL_G)/LL_C$		
			Value	10 ⁶ err	10 ⁶ res	Value	10 ⁴ err	10 ⁴ res
36.415	0.07785	0.07251	0.15037	44	-32	0.0709	82	120
36.411	0.07836	0.07213	0.15049	19	-19	0.0827	34	-49
36.410	0.07887	0.07194	0.15081	19	12	0.0920	33	-6
36.408	0.07919	0.07156	0.15074	17	6	0.1013	29	2
36.367	0.08223	0.06849	0.15072	10	1	0.1823	15	-13
36.291	0.08501	0.06574	0.15075	10	1	0.2557	13	24
36.127	0.08822	0.06260	0.15082	9	2	0.3401	13	15
36.013	0.08986	0.06106	0.15091	9	7	0.3822	12	22
34.900	0.09819	0.05300	0.15119	9	-8	0.5997	12	-27
32.540	0.10746	0.04471	0.15217	9	-3	0.8328	12	-25
30.426	0.11308	0.03996	0.15304	9	1	0.9705	12	-15
28.464	0.11733	0.03644	0.15377	9	-3	1.0737	12	9
26.130	0.12162	0.03310	0.15473	9	1	1.1749	12	15
25.315	0.12291	0.03206	0.15496	9	-7	1.2058	12	9
24.125	0.12480	0.03068	0.15548	9	-2	1.2492	12	8
23.825	0.12523	0.03048	0.15571	9	10	1.2575	12	-11
$T_c = 36.417$			$2LL_C = 0.15068$			$\ln 2B_1 = 1.3454$		
			± 2			± 25		
			Slope $a = 0.121$			$B_1 = 1.920$		
			± 1			$\beta_1 = 0.3482$		
			$a^* = a/2LL_C = 0.80$			± 7		
			s.d. = 0.63			s.d. = 1.39		

is confirmed by fitting with a variety of values of α . The standard deviation decreases when α turns negative (Fig. 4). Since this run contains relatively few points, and since there is some trouble with some of these (Sec. VII), too much should not be read into these results.

B. CO₂ Series II

A typical deviation plot for fitting $LL_L + LL_G$ to a straight line using all points and taking $T_c = 30.991^\circ\text{C}$ is shown in Fig. 3. All points are within two times their estimated error from the straight line. There are

TABLE VII. CClF₃ 99.34% pure.

Temperature (°C)	LL_L	LL_G	$(LL_L + LL_G)$			$(LL_L - LL_G)/LL_C$		
			Value	10 ⁶ err	10 ⁶ res	Value	10 ⁴ err	10 ⁴ res
28.685	0.07047	0.06016	0.13063	10	-3	0.1579	17	-16
28.650	0.07213	0.05861	0.13074	10	7	0.2069	15	30
28.473	0.07563	0.05507	0.13070	9	-4	0.3147	14	-38
27.860	0.08166	0.04932	0.13097	9	0	0.4951	14	-5
26.770	0.08734	0.04400	0.13133	9	-4	0.6635	14	14
25.035	0.09325	0.03885	0.13210	9	8	0.8327	14	33
21.770	0.10044	0.03278	0.13321	9	-3	1.0357	14	-25
$T_c = 28.720^\circ\text{C}$			$2LL_C = 0.13065$			$\ln 2B_1 = 1.3726$		
			± 3			± 84		
			Slope $a = 0.112$			$B_1 = 1.972$		
			± 3			$\beta_1 = 0.3540$		
			$a^* = a/2LL_C = 0.86$			± 18		
			s.d. = 0.60			s.d. = 2.1		

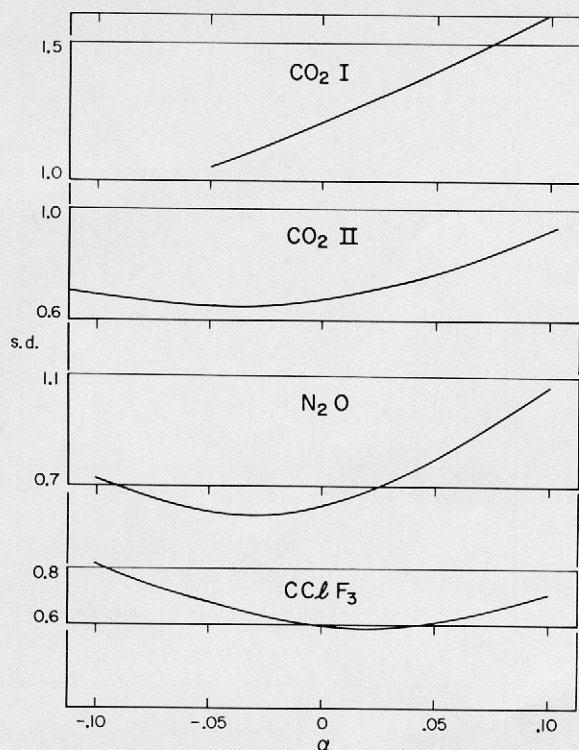


Fig. 4. Standard deviation of the fit $LL_L + LL_G = 2LL_G(1 + B_2|t|^{1-\alpha})$ for various choices of α and for the four sets of data. If anything, a slightly negative value of α seems to be favored.

sufficient data to vary the range. Slope and intercept of the straight line behave as shown in Table VIII, and are essentially constant within their error. If functions of the form $|t|^{1-\alpha}$ are admitted, the standard deviation shows a tendency to decrease with decreasing α , favoring slightly negative values of this quantity (Fig. 4).

C. N₂O

Fitting the sum $LL_L + LL_G$ for all 16 data points results in the deviation plot Fig. 3. The points are fitted roughly within one standard deviation. On varying the

TABLE VIII. Diameter of CO₂ Series II, $T_c = 30.991^\circ\text{C}$. Vary range.

T min ($^\circ\text{C}$)	$ t _{\max}$ (%)	$2LL_G$	s.d.	Slope	s.d.
21.508	3.12	0.140958 ± 0.000018		0.1161 ± 0.0016	
25.480	1.81	0.140967 ± 0.000019		0.1128 ± 0.0028	
27.828	1.04	0.140970 ± 0.000022		0.1115 ± 0.0054	
29.115	0.62	0.140974 ± 0.000025		0.1065 ± 0.0107	
30.312	0.223	0.140969 ± 0.000032		0.1175 ± 0.0330	
30.662	0.108	0.140977 ± 0.000040		0.0899 ± 0.0722	
30.833	0.052	0.140975 ± 0.000054		0.1006 ± 0.200	

temperature range, one obtains intercepts and slopes as shown in Table IX. They are constant within error.

The standard deviation of the fit again decreases slightly if forms like $|t|^{1-\alpha}$, with α slightly negative, are tried. This is shown in Fig. 4.

D. CClF₃

The seven values of $LL_L + LL_G$ are fitted by a straight line perfectly; see the deviation plot Fig. 3. In view of the scarcity of data, the range could not be varied appreciably. Admitting a form $|t|^{1-\alpha}$, the standard deviation is minimal for α slightly positive (Fig. 4).

E. Conclusions

We conclude that the present data agree with the hypothesis of a straight diameter within their level of accuracy (1×10^{-4} in n , 0.001° in T). If the diameter is described by $|t|^{1-\alpha}$, the data seem slightly biased towards negative values of α . These conclusions do not

TABLE IX. Diameter of N₂O, $T_c = 36.417^\circ\text{C}$. Vary range.

T min ($^\circ\text{C}$)	$ t _{\max}$ (%)	$2LL_G$	s.d.	Slope	s.d.
23.835	4.06	0.150683 ± 0.000024		0.1213 ± 0.0010	
25.315	3.59	0.150691 ± 0.000023		0.1201 ± 0.0012	
28.464	2.57	0.150691 ± 0.000025		0.1199 ± 0.0021	
32.540	1.25	0.150699 ± 0.000028		0.1158 ± 0.0054	
36.013	0.130	0.150675 ± 0.000041		0.1751 ± 0.053	
36.291	0.041	0.150674 ± 0.000067		0.1906 ± 0.25	

depend on the choice of T_c since the behavior of $LL_L + LL_G$ is quite insensitive to this choice. Best values for slope and intercept are summarized in Tables IV-VII. It is seen that the reduced slope $a^* = (B_2^+ + B_2^-)/2$ is of order unity.

It is not possible, from the present set of data, to resolve the question whether, in (5), $B_2^+ = B_2^-$. There is a strong indication, however, that they are of about the same size. In forming the difference, $LL_L - LL_G$, we will find (Sec. VII) that the leading term in the expansion (5) fits the data over the entire range of temperatures. For gases like Ar, for which a larger temperature range is available, we have found¹⁸ that the asymptotic range for the difference $\rho_L - \rho_G$ is approximately 9% in t . However, in fitting gas and liquid sides separately, the asymptotic range is no more than 0.3% in t . Consequently, the next terms in the expansion, $B_2^+ |t|^{\beta_2^+}$ and $B_2^- |t|^{\beta_2^-}$, must nearly cancel out when the difference is taken.

VII. BEST VALUES OF B_1 , β_1 , B_2

After assigning weights (Sec. IV) the sum $LL_L + LL_G$ was fitted to a straight line over the whole range of

temperature (0.04 in t). The best value of the intercept $2 LL_C$ so obtained was independent of the choice of T_c ; it was used to reduce the difference $LL_L - LL_G$. The reduced difference was then fitted as follows:

$$\ln[(LL_L - LL_G)/LL_C] = \ln 2B_1 + \beta_1 \ln |t|. \quad (12)$$

The fit was performed for several values of T_c . In the cases of CO_2 and N_2O we found that a minimum standard deviation occurred for T_c at most 0.001° from that observed directly. In CClF_3 for which no data very near critical were taken, the minimum standard deviation occurred for T_c 0.005° above the observed value. The values of LL_L , LL_G , the sum, the reduced difference, the estimated errors, and the residual of the fits are listed in Tables IV–VII for the four data sets. Also, optimum values for T_c , LL_C , the slope, B_1 , and β_1 are given with their respective standard deviations. The standard deviations of all the fits are seen to be near unity. The residuals of the fits are plotted in Fig. 5. Most points are fitted within one or two times their estimated standard deviation. In the case of CO_2 , series I, we had to reject the points at 30.974 and 29.792°C because they were out by six and four standard deviations, respectively, when fitting the difference.

The coefficient B_1 varies little, from 1.920 for N_2O to 1.972 for CClF_3 . The values found for β_1 lie between 0.345 and 0.354. However, taking into account the changes in β_1 on varying T_c and range for a single substance, the conclusion that β_1 depends on the substance seems unwarranted. The reduced slopes are all between 0.8 and 0.9.

We have made sure that the optimum values thus obtained are independent of the range. The fits were repeated decreasing the value of $|t|_{\max}$. The results are summarized in Tables X and XI. Although, for CO_2 Series II, we note a decrease in β_1 slightly exceeding the error (0.348 to 0.342 for $|t|_{\max}$ from 3% to 0.2%), in all other cases there are no variations appreciably exceeding the error. From the refractive index data alone we conclude that the expression $(LL_L - LL_G)/LL_C = 2B_1 |t|^{\beta_1}$ is valid within error over 0.04 in t . From other coexistence curves¹⁸ extending over larger ranges, it is found that $|t|_{\max}$ may be around 0.09 for the asymptotic expression.

VIII. THE EFFECT OF IMPURITIES

In addition to the data on pure substances, for N_2O two runs with known amounts of impurities were made, namely, one with 0.39 mole % air and one with 1.1 mole % water.

The air impurity will be present in the gas phase mainly, while the water impurity will tend to concentrate in the liquid phase. The change in refractive index occurring when the temperature is raised is partly due to redistribution of the impurity between the phases. It is interesting to investigate how the critical behavior

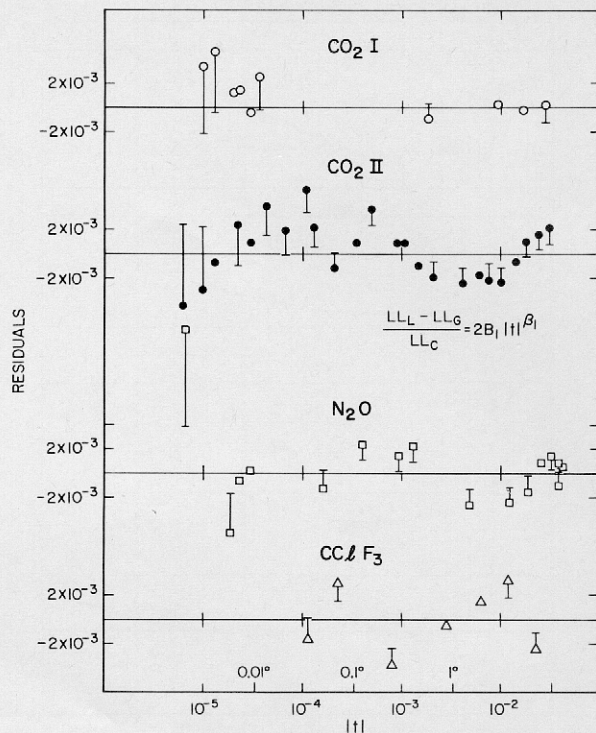


FIG. 5. Residuals of the fit $(LL_L - LL_G)/LL_C = 2B_1 |t|^{\beta_1}$ for the four sets of data. Bars denote estimated errors of the experimental data.

is affected by impurities. We have analyzed the data exactly as those for pure substances. The results are shown in Tables XII and XIII. The critical temperature is defined as the temperature at which the refractive indices become equal when the filling density is such that the meniscus disappears in the center of the cell. Experimentally, it was observed in the case of the air impurity to be about 36.164°C . Fitting the data for the difference, we find that the standard deviation is minimal at 36.174° , compared to 36.417° for pure N_2O (Table XII). This large change in the value of T_c , 0.24° for 0.4% impurity, does not affect the values of B_1 and β_1 greatly, as is seen in Table XIV.

The results of the fit for the case of the water impurity are shown in Table XIII. Here, the critical temperature is slightly increased (to 36.494°), but again, the value of β_1 is almost unchanged. However, the coefficient B_1 shows a sizeable change (Table XIV). We conclude that the prime effect of impurities is a change of T_c ; although the coefficient B_1 may be affected by their presence, the exponent β_1 is quite insensitive to impurities. Although exponent renormalization is in general expected for a gas-liquid system with constant over-all impurity content,¹⁹ our dilution parameter $|T_c^0 - T_c|/T_c^0$, being smaller than 10^{-3} , is not large enough to make renormalization experimentally visible.²⁰

TABLE X. Vary range of t . CO₂ Series I and II.

Substance	$ t _{\max}$ (%)	$LL_L + LL_G$			$(LL_L - LL_G)/LL_C$		
		s.d.	$2LL_C$	Slope	s.d.	$\ln 2B$	β
CO ₂ I $T_c = 31.030^\circ\text{C}$	2.72	1.22	0.13915 ± 7	0.121 ± 5	0.62	1.353 ± 3	0.3450 ± 6
	1.76	1.11	0.13918 ± 7	0.112 ± 7	0.65	1.351 ± 4	0.3448 ± 8
	0.85	0.71	0.13925 ± 5	0.084 ± 10	0.70	1.350 ± 6	0.3447 ± 12
CO ₂ II $T_c = 30.991^\circ\text{C}$	3.12	0.68	0.14096 ± 2	0.116 ± 2	1.42	1.364 ± 3	0.3475 ± 6
	1.81	0.68	0.14097 ± 2	0.113 ± 3	1.29	1.358 ± 4	0.3463 ± 7
	1.04	0.71	0.14097 ± 2	0.111 ± 5	1.04	1.347 ± 4	0.3447 ± 7
	0.61	0.74	0.14097 ± 2	0.107 ± 11	1.04	1.340 ± 6	0.3437 ± 10
	0.22	0.80	0.14097 ± 3	0.117 ± 33	1.00	1.327 ± 11	0.3418 ± 16
	0.11	0.85	0.14098 ± 4	0.090 ± 72	1.05	1.339 ± 18	0.3433 ± 24
	0.052	0.93	0.14098 ± 5	0.10 ± 0.20	1.13	1.352 ± 35	0.3449 ± 42
	0.021	0.78	0.14087 ± 6	1.3 ± 5	1.05	1.264 ± 69	0.3352 ± 77

TABLE XI. Vary range of t . N₂O and CClF₃.

Substance	$ t _{\max}$ (%)	$LL_L + LL_G$			$(LL_L - LL_G)/LL_C$		
		s.d.	$2LL_C$	Slope	s.d.	$\ln 2B$	β
N ₂ O $T_c = 36.417^\circ\text{C}$	4.1	0.63	0.15068 ± 2	0.121 ± 1	1.39	1.345 ± 2	0.3482 ± 7
	3.6	0.58	0.15069 ± 2	0.120 ± 1	1.47	1.346 ± 3	0.3483 ± 8
	2.6	0.61	0.15069 ± 2	0.120 ± 2	1.47	1.342 ± 4	0.3476 ± 9
	1.25	0.64	0.15070 ± 3	0.116 ± 5	1.29	1.332 ± 6	0.3459 ± 11
	0.13	0.60	0.15067 ± 4	0.18 ± 5	1.05	1.371 ± 22	0.3511 ± 31
	0.041		0.15067 ± 7	0.19 ± 0.26		1.426 ± 57	0.3576 ± 69
CClF ₃ $T_c = 28.720^\circ\text{C}$	2.3		0.13065 ± 3	0.112 ± 3		1.373 ± 8	0.3540 ± 18
	1.2		0.13064 ± 3	0.117 ± 5		1.387 ± 10	0.3564 ± 20
	0.65		0.13066 ± 3	0.106 ± 10		1.383 ± 18	0.3558 ± 31

TABLE XII. N₂O. 0.39% air impurity.

Temperature (°C)	LL_L	LL_G	(LL_L+LL_G)			$(LL_L-LL_G)/LL_C$		
			Value	10 ⁵ err	10 ⁵ res	Value	10 ⁴ err	10 ⁴ res
35.728	0.08967	0.06074	0.15040	9	12	0.3855	12	2
34.978	0.09575	0.05468	0.15044	9	-14	0.5472	12	3
33.962	0.10093	0.04996	0.15090	9	-7	0.6791	12	-9
32.021	0.10777	0.04400	0.15176	9	4	0.8497	12	-3
29.528	0.11413	0.03866	0.15279	9	9	1.0056	12	16
25.836	0.12113	0.03297	0.15410	9	-3	1.1746	12	5
23.280	0.12517	0.02996	0.15512	9	-1	1.2685	12	11
$T_c=36.174^\circ\text{C}$			$2LL_C=0.15011$			$\ln 2B_1=1.3643$		
			± 6			± 21		
			Slope $a=0.121$			$B_1=1.957$		
			± 3			$\beta_1=0.3542$		
			$a^*=a/2LL_C=0.81$			± 5		
			s.d.=1.08			s.d.=0.82		

IX. THE MICHELS DATA FOR CO₂

The coexisting densities reported by Michels *et al.*⁹ and summarized in Table XV were obtained by extrapolating isothermal PV data to the density at which the pressure equals the vapor pressure. Since isotherms near critical are very flat, the error in the density values at the intercept becomes large. This presents a rather complicated weighting problem. The experiment was carried out in a bomb of sizeable vertical dimensions. Thus we expect the highest point, at 31.01°C, to be beset with a large density gradient due to gravity and have therefore excluded it from the analysis. From experience with other substances, we expect the point at 2°C ($t=0.095$) to be borderline as

far as the asymptotic behavior $\Delta\rho=B_1\pm|t|^{\beta_1}$ is concerned and have therefore excluded it from the fit. If it is included it is always out by several standard deviations.

In the absolute weight assignment, we have accounted for errors in density, temperature, and pressure along the isotherm, for errors in temperature and pressure along the vapor pressure curve, and for the declining slope of the isotherms when the critical point is approached. We have not accounted for the error in extrapolating the isotherms. The variance of the density along an isotherm due to errors in ρ , P , T is, by propagation of error,

$$\text{Var}_{\text{isoth}}\{\rho\}=\sigma_\rho^2+(\partial\rho/\partial T)^2_P\sigma_T^2+(\partial\rho/\partial P)^2_T\sigma_P^2. \quad (13)$$

TABLE XIII. N₂O. 1.1% water impurity.

Temperature (°C)	LL_L	LL_G	(LL_L+LL_G)			$(LL_L-LL_G)/LL_C$		
			Value	10 ⁵ err	10 ⁵ res	Value	10 ⁴ err	10 ⁴ res
36.101	0.08916	0.06119	0.15035	9	-9	0.4793	16	-6
35.170	0.09700	0.05391	0.15091	9	12	0.7383	16	32
34.198	0.10162	0.04958	0.15120	9	4	0.8916	16	-2
32.274	0.10808	0.04367	0.15175	9	-13	1.1035	16	-9
30.387	0.11296	0.03963	0.15260	9	0	1.2562	16	-11
28.459	0.11708	0.03637	0.15346	9	+13	1.3828	16	-17
26.510	0.12058	0.03343	0.15401	9	-5	1.4931	16	-11
24.583	0.12376	0.03101	0.15477	9	-1	1.5891	16	-6
22.737	0.12663	0.02884	0.15547	9	-1	1.6753	16	32
$T_c=36.494$			$2LL_C=0.15029$			$\ln 2B_1=1.6073$		
			± 5			± 28		
			Slope $a=0.117$			$B_1=2.50$		
			± 2			$\beta_1=0.3511$		
			$a^*=a/2LL_C=0.78$			± 7		
			s.d.=1.02			s.d.=1.23		

TABLE XIV. The effect of impurities.

Substance	T_c (°C)	s.d. of		s.d.	β_1	s.d.
		fit	$\ln 2B_1$			
Pure N ₂ O	36.417	1.39	1.3454±0.0025	0.3482±0.0007		
N ₂ O, 0.39% air	36.174	0.82	1.3643±0.0021	0.3542±0.0005		
	(36.164)	0.93	1.3596±0.0023	0.3528±0.0006		
N ₂ O, 1.1% H ₂ O	36.494	1.23	1.6073±0.0028	0.3511±0.0007		
	(36.484)	1.42	1.6028±0.0032	0.3498±0.0009		

Similarly, for the vapor pressure

$$\text{Var}\{P_{\text{vap}}\} = \sigma_P^2 + (dP/dT)^2_{\text{vap}} \sigma_T^2. \quad (14)$$

Then, the variance of the intercept is readily seen to be

$$\text{Var}\{\rho_{\text{coex}}\} = \text{Var}\{\rho_{\text{isoth}}\} + \text{Var}\{P_{\text{vap}}\} (\partial\rho/\partial P)^2_T. \quad (15)$$

It may be written as

$$\text{Var}\{\rho_{\text{coex}}\} = \text{Var}_{\text{coex}}\{\rho\rho\} + \text{Var}_{\text{coex}}\{\rho T\} + \text{Var}_{\text{coex}}\{\rho P\}, \quad (16)$$

where

$$\begin{aligned} \text{Var}_{\text{coex}}\{\rho\rho\} &= \sigma_\rho^2, \\ \text{Var}_{\text{coex}}\{\rho T\} &= (\partial\rho/\partial P)^2_T [(\partial P/\partial T)^2_\rho + (dP/dT)^2_{\text{vap}}] \sigma_T^2, \\ \text{Var}_{\text{coex}}\{\rho P\} &= 2(\partial\rho/\partial P)^2_T \sigma_P^2. \end{aligned}$$

Here σ_ρ , σ_T , σ_P have to be estimated from the experimental precision. We have assumed $\sigma_T = 0.006^\circ\text{C}$, $\sigma_P = 10^{-3}$ atm, $\sigma_\rho = 2 \times 10^{-2}$ amagat. The derivatives are directly obtained from the experimental PVT data. Since $(\partial\rho/\partial P)_T$ diverges at the critical point, $\text{Var}\{\rho T\}$ and $\text{Var}\{\rho P\}$ become large for data close to critical; $\text{Var}\{\rho T\}$ dominates. The estimated errors of the individual points are shown in Table XVI.

Once the variance of the coexisting densities is obtained, the absolute weight of $\rho_L + \rho_G$ is given by

$$w\{\rho_L + \rho_G\} = [\text{Var}\{\rho_L\} + \text{Var}\{\rho_G\}]^{-1} \quad (17)$$

with $\text{Var}\{\rho_L\}$, $\text{Var}\{\rho_G\}$ from (16). Similarly the weight of $\ln[(\rho_L - \rho_G)/\rho_C]$ is given by

$$w\{\ln[(\rho_L - \rho_G)/\rho_C]\} = (\rho_L - \rho_G)^2 / (\text{Var}\{\rho_L\} + \text{Var}\{\rho_G\}). \quad (18)$$

Error estimates for $\rho_L + \rho_G$, $(\rho_L - \rho_G)/\rho_C$ are readily obtained from these weights. Since $\text{Var}\{\rho_L\}$ and $\text{Var}\{\rho_G\}$ become large near critical, the error in $(\rho_L - \rho_G)/\rho_C$ also increases markedly when $|t|$ becomes small.

We experienced considerable difficulty in fitting the data. On fitting the sum, the point at 19.874° was always out by several standard deviations. Not finding any physical reason for rejecting it, we have presented fits with and without this point. On varying the value of T_c , the fit improves markedly when T_c is decreased below the literature value of 31.04°C . However, the

residual of the highest point became very large at the same time. Thus we present three fits, each of which is for optimized T_c . These are fits to all seven points from 10.8 – 30.4° , to six points, 30.4° omitted, and to six points, 19.9° omitted, respectively (Table XVII). Although the quality of the fits leaves much to be desired, the values of ρ_c , slope, B_1 , and β_1 do not vary much. A fair average is shown in Table XVIII which also includes a comparison with the optical data.

The intercomparison between the optical and the PVT data is rather revealing. The values of β_1 obtained by these two vastly different methods in different temperature ranges are in fine agreement. In comparing T_c values from optical and PVT data it should be noted that the value of T_c reported by Michels *et al.*⁹ is valuable only within the framework of their own data, since their temperature scale is not well defined with respect to I.P.T.S. However, the optimum values of T_c obtained by us for Michels' coexistence curve are considerably lower than the value 31.05°C they report as the point at which liquid and vapor densities become equal. The difference between their and our result may be due to the fact that they included the point at 31.01°C and, most likely, gave all points equal weight. In the optical experiments, the value of T_c is determined directly. The difference in T_c of 0.04° for the two samples must be due to small impurities. (See also Sec. VIII.)

There are small differences in B_1 between Michels' and the refractive index data which we feel to be within reason, in view of the spread in B_1 of the optical data. The differences in slope, however, seem to be real; they are probably caused by ignoring the density dependence of the function LL/ρ (cf. Sec. III). The experimental data for the dielectric constant and refractive index of CO₂¹² indicate that $(\epsilon - 1)/(\epsilon + 2)\rho$ and $(n^2 - 1)/(n^2 + 2)\rho$ pass through a maximum at densities slightly higher than critical. Thus, the sum of $LL_L + LL_G$ at $\rho_G = 100$ amagat, $\rho_L = 400$ amagat ($\sim 20^\circ\text{C}$) is about 0.5% lower than its value at the average density 250 amagat. Since the value of $LL_L + LL_G$ varies by only 3% between the critical point and

TABLE XV. Coexistence curve of CO₂, Michels' data.^a

t (°C)	ρ_L (amagats)	ρ_G (amagats)
[2.853	461.8	54.04]
10.822	433.6	70.21
19.874	393.0	97.62
25.070	359.8	122.67
25.298	357.7	124.47
28.052	331.7	146.46
29.929	301.0	172.30
30.409	290.3	182.22
[31.013	259.0	216.4]

^a A. Michels, B. Blassie, and C. Michels, Proc. Roy. Soc. (London) **A902**, 358 (1937).

TABLE XVI. Estimated errors of coexisting densities of CO₂, Eqs. (15), (16).

Temperature	(Var{ $\rho\rho$ }) ^{1/2}	(Var{ ρT }) ^{1/2}	(Var{ ρP }) ^{1/2}	Estimated error in ρ	ρ (amagats)
2.853	0.02	0.030	0.001	0.036	461.8
10.822	0.02	0.032	0.001	0.037	433.6
19.874	0.02	0.042	0.002	0.046	393.0
25.070	0.02	0.083	0.005	0.086	359.8
25.298	0.02	0.092	0.006	0.094	257.7
28.052	0.02	0.16	0.012	0.159	331.7
29.929	0.02	0.67	0.056	0.67	301.0
30.409	0.02	0.94	0.080	0.94	290.3
2.853	0.02	0.015	0.004	0.025	54.04
10.822	0.02	0.022	0.004	0.030	70.21
19.874	0.02	0.049	0.008	0.054	97.62
25.070	0.02	0.095	0.013	0.098	122.67
25.298	0.02	0.098	0.014	0.101	124.47
28.052	0.02	0.16	0.020	0.16	146.46
29.929	0.02	0.53	0.061	0.53	172.30
30.409	0.02	0.61	0.069	0.62	182.22

TABLE XVII. Fit coexistence curve CO₂ (Michels).

t (°C)	$\rho_L + \rho_G$ (amagats)			$(\rho_L - \rho_G)/\rho$		
	Value	Err.	Res.	Value	Err.	Res.
10.822	503.81	0.05	-0.04	1.5337	0.0002	-0.0001
19.874	490.62	0.07	0.23	1.2466	0.0003	0.0007
25.070	482.47	0.13	-0.20	1.0008	0.0005	0.0008
25.298	482.17	0.14	-0.16	0.9843	0.0006	-0.0020
28.052	478.16	0.23	-0.08	0.7818	0.0010	-0.0010
29.929	473.30	0.86	-2.14	0.5432	0.0036	-0.0045
30.409	472.52	1.13	-2.21	0.4561	0.0047	0.0136
Optimum T_c 30.98°C						
$2\rho_c = 473.85 \pm 0.22$			$\ln 2B_1 = 1.3739 \pm 0.0020$			
Slope $a = 452 \pm 4$			$B_1 = 1.975^a$			
$a^* = a/2\rho_c = 0.95^b$			$\beta_1 = 0.3486 \pm 0.0006^b$			
s.d. = 2.22			s.d. = 2.46 (min)			
10.822	503.81	0.05	-0.04	1.5333	0.0002	0.0000
19.874	490.62	0.07	0.22	1.2464	0.0003	0.0003
25.070	482.47	0.13	-0.21	1.0006	0.0005	0.0008
25.298	482.17	0.14	-0.17	0.9841	0.0006	-0.0019
28.052	478.16	0.23	-0.09	0.7816	0.0010	0.0007
29.929	473.30	0.86	-2.16	0.5431	0.0036	0.0027
Optimum T_c 30.92°C						
$2\rho_c = 473.99 \pm 0.22$			$\ln 2B_1 = 1.3690 \pm 0.0016$			
Slope $a = 452 \pm 4$			$B_1 = 1.966$			
$a^* = a/2\rho_c = 0.95^b$			$\beta_1 = 0.3466 \pm 0.0005$			
s.d. = 2.29			s.d. = 1.95 (min)			
10.822	503.81	0.05	-0.002	1.5346	0.0002	0.0000
25.070	482.47	0.13	-0.003	1.0014	0.0005	0.0075
25.298	482.17	0.14	0.038	0.9849	0.0006	-0.0013
28.052	478.16	0.23	0.15	0.7823	0.0010	-0.0008
29.929	473.30	0.86	-1.90	0.5435	0.0036	-0.0059
30.409	472.52	1.13	-1.96	0.4564	0.0048	0.0102
Optimum T_c 31.00°C						
$2\rho_c = 473.59 \pm 0.17$			$\ln 2B_1 = 1.3773 \pm 0.0020$			
Slope $a = 456 \pm 3$			$B_1 = 1.982$			
$a^* = a/2\rho_c = 0.96^d$			$\beta_1 = 0.3498 \pm 0.0007$			
s.d. = 1.45			s.d. = 2.28 (min)			

TABLE XVIII. Parameters of the coexistence curve of CO₂. Averages are for fits with varying sets of data points (Table XVII). Errors indicated span extremes among these fits.

Michels	Refractive index	
	CO ₂ I	CO ₂ II
$\rho_c = 236.9 \pm 0.2$ amagats		
Reduced slope $= 0.96 \pm 0.01$	0.87	0.82
$\ln 2B_1 = 1.373 \pm 0.004$	1.3528	1.3642
$B_1 = 1.974 \pm 0.008$	1.935	1.957
$\beta_1 = 0.348 \pm 0.002$	0.3450	0.3475
$T_c = 30.97 \pm 0.05^\circ\text{C}$	31.030	30.991

20°C we expect the reduced slope of $LL_L + LL_G$ to be about 15% lower than that of $\rho_L + \rho_G$. In agreement with this, our analysis gives 0.85 for the slope of the optical data and 0.96 for that of the Michels data.

X. THE COOK DATA FOR N₂O

The coexisting densities of N₂O reported by Cook and summarized in Table XIX were determined in a glass burette filled with a known amount of gas and sealed with mercury. The liquid volumes were obtained by decreasing the pressure on the compressed liquid until a small gas bubble formed. Similarly, the gas volumes were obtained by increasing the pressure on the unsaturated gas until the liquid first appeared. The burette was calibrated using the coexisting densities of CO₂ determined by Michels; temperature control and measurement were to 0.01°C.

Absolute weight assignment was achieved by assuming that density determinations were subject to error characterized by a standard deviation σ_ρ (not necessarily independent of ρ) while temperature measurements have a characteristic standard deviation σ_T . Using propagation of error, we then have

$$\text{Var}\{\rho\} = \text{Var}\{\rho\rho\} + \text{Var}\{\rho T\}, \quad (19)$$

where $\text{Var}\{\rho\rho\}$ is simply equal to σ_ρ^2 . $\text{Var}\{\rho T\}$ is obtained using the asymptotic relation between a saturation density ρ and temperature: $|\rho - \rho_c| = B_1 |t|^{\beta_1}$, as follows

$$\text{Var}\{\rho T\} = [\beta \sigma_T (\rho - \rho_c) / (T - T_c)]^2. \quad (20)$$

From (19) and (20) errors and weights of quantities of interest are obtained. For instance, the weight assigned to $\ln[(\rho - \bar{\rho})/\rho_c]$, $\bar{\rho}$ being the density at the diameter, is given by

$$w \left\{ \ln \left[\frac{(\rho - \bar{\rho})}{\rho_c} \right] \right\} = \left[\left(\frac{\sigma_\rho}{\rho - \bar{\rho}} \right)^2 + \left(\frac{\beta \sigma_T}{T - T_c} \right)^2 \right]^{-1}. \quad (21)$$

Even if σ_ρ , σ_T are constant, the weight assigned to points near critical decreases rapidly due mainly to the temperature-dependent term in (21). This fact is often overlooked in graphical log-log analyses of coexistence curves.

In fitting the Cook data we have assumed that

$\sigma_T = 0.01^\circ$, $\sigma_\rho = 10^{-3}\rho$ (constant relative error). We have obtained best values for the diameter by fitting all sums of coexisting densities. The best value of ρ_c so obtained was used to reduce the density differences. Since pairs of densities were not obtained at all temperatures, we have followed the practice of fitting $|\rho - \bar{\rho}| = B_1 |t|^{\beta_1}$, where $\bar{\rho}$ is the value of the diameter calculated at t . The results of the fits are summarized in Table XX. Since the closest point is over 2° from critical, the fit is not very sensitive to the choice of T_c . A minimum standard deviation in the fit of the difference is obtained for T_c about 36.34°C; the standard deviation increases by 10% when T_c is varied by 0.12°C around the optimum. The best parameters, and their variations when T_c changes by 0.12°C, are shown in Table XXI and compared with the best values derived from the München data. Except for the slope, the agreement between the two sets of data is as good as could be desired. The apparent low slope of the refractive index data may have the same explanation as in the case of CO₂, namely that the Lorentz-Lorenz function LL/ρ goes through a maximum near the critical density and is lower both in gas and liquid phase below T_c .

XI. DISCUSSION AND CONCLUSIONS

Refractive index data, recently obtained in the coexisting phases of CO₂, N₂O, and CClF₃, are particularly useful for studying the asymptotic behavior of the coexistence curve near the critical point. Unlike more classical methods in which bulk densities are determined, refractive index determinations probe a thin slab of fluid right near the interface; thus they are not

TABLE XIX. Coexistence curve of N₂O. Cook's data.^a

Temperature (°C)	ρ_L (g/cm ³)	ρ_G (g/cm ³)
20.00	0.789	0.159
21.00	0.782	
22.00	0.775	0.171
23.00	0.766	
24.00	0.752	0.183
25.00	0.746	0.190
26.00	0.731	0.197
27.00	0.723	0.205
28.41		0.218
28.45	0.707	
30.00	0.689	0.234
31.00	0.671	0.246
32.00	0.655	0.260
33.00	0.638	0.277
34.00		0.295
34.02	0.617	
36.39		

^a D. Cook, Trans. Faraday Soc. **49**, 716 (1953).

TABLE XX. Fit coexistence curve of N₂O (Cook).

Temperature	$\rho_L + \rho_G = 2\rho$	Err.	Res.	$(\rho_L - \bar{\rho})/\rho_c$	Err.	Res.	$(\bar{\rho} - \rho_G)/\rho_c$	Err.	Res.
20.00	0.948	0.0016	0.0001	0.6970	0.0035	0.0003	0.6967	0.0007	0.0000
21.00				0.6845	0.0035	0.0030			
22.00	0.946	0.0016	0.0035	0.6720	0.0034	0.0064	0.6642	0.0008	0.0014—
23.00				0.6550	0.0034	0.0060			
24.00	0.935	0.0016	0.0021—	0.6270	0.0033	0.0046—	0.6317	0.0008	0.0001
25.00	0.936	0.0015	0.0015	0.6167	0.0032	0.0034	0.6133	0.0009	0.0000
26.00	0.928	0.0015	0.0038—	0.5865	0.0032	0.0073—	0.5948	0.0009	0.0010
27.00	0.928	0.0015	0.0011—	0.5718	0.0031	0.0013—	0.5742	0.0009	0.0011
28.41							0.5412	0.0010	0.0000—
28.45				0.5407	0.0031	0.0034			
30.00	0.923	0.0015	0.0019	0.5054	0.0030	0.0049	0.5011	0.0011	0.0005
31.00	0.917	0.0014	0.0014—	0.4686	0.0030	0.0029—	0.4716	0.0011	0.0001
32.00	0.915	0.0014	0.0007—	0.4362	0.0029	0.0024—	0.4377	0.0012	0.0008—
33.00	0.915	0.0014	0.0020	0.4015	0.0029	0.0013	0.3971	0.0013	0.0031—
34.00							0.3543	0.0014	0.0008
34.02				0.3581	0.0028	0.0057			
2ρ _c = 0.90406 ± 0.00176				Optimum T _c = 36.34					
Slope a = 0.830 ± 0.055				ln B ₁ = 0.6655 ± 0.0044					
Red. slope a* = a/2ρ _c = 0.92				B ₁ = 1.945 ± 0.007					
				β ₁ = 0.3491 ± 0.0013					
s.d. = 1.55				s.d. = 1.24					

affected by the presence of density gradients set up by gravity in the highly compressible medium, except for some curvature of the beam which is negligible up to a few millidegrees from the critical point. A second advantage, shared with other methods of visual observation, is the direct determination of the critical temperature. Furthermore, the analysis was simplified by the fact that liquid and gas densities were determined at the same temperature. A drawback of the method is that refractive indices have to be converted to densities. However, we have shown that the use of the Lorentz-Lorenz relation introduces only small errors in the analysis.

In the data analysis, weight assignment had to be done with care since even small temperature errors cause large density variations when the critical point is approached. Standard deviations of 0.001°C in temperature and 0.0001 in refractive index were assumed

and propagation of error was used to estimate errors in, and give absolute weight assignment to, quantities of interest such as $LL = (n^2 - 1)/(n^2 + 2)$, $LL_L + LL_G$, etc.

The questions we have tried to answer are those regarding the asymptotic behavior of the coexistence curve, and the form of the next term, in the nonclassical expansion $LL - LL_G = B_1^\pm |t|^{\beta_1^\pm} + B_2^\pm |t|^{\beta_2^\pm} \dots$, where + refers to the liquid and - to the gas. We have fitted the data using the leading term only and decreasing the range of $|t|$; the asymptotic expression fits the $LL - LL_G$ data within their estimated error only for $|t|_{\max} < 0.003$ and it is symmetric, i.e., $B_1^+ = -B_1^-$, $\beta_1^+ = \beta_1^-$, within their combined standard deviations of about 3% in B_1 and 1½% in β_1 . However, on forming the difference $LL - LL_G$, the asymptotic expression is found to be valid over the full range of the present data, $|t|_{\max} = 0.04$; in fact, from other data extending over larger ranges $|t|_{\max}$ is found to be as large as 0.09. This indicates that there is near-cancellation of higher-order terms, and since it is plausible that β_2^+ and β_2^- are the same, the coefficients B_2^+ and B_2^- cannot be very different. Assuming equality of β_2^+ and β_2^- , some conclusions can be drawn from the present data on the values of $B_2^+ + B_2^-$ and of β_2 . This is done by forming the sum $LL_L + LL_G$ in which the leading term in the expansion drops out. The sum varies only a few percent over the range of the present data, about 10° below T_c , and its temperature dependence is in accordance with the law of the rectilinear diameter, i.e., a straight line fits the data on the sum to within one

TABLE XXI. Parameters of the coexistence curve of N₂O. Errors indicate parameter change for ±0.12° in T_c.

Cook	Refractive index
ρ _c = 0.452 ± 0.001	
Reduced slope = 0.92 ± 0.07	0.80
ln B ₁ = 0.666 ± 0.017	
B ₁ = 1.95 ± 0.03	1.920
β ₁ = 0.349 ± 0.006	0.348
T _c = 36.34 ± 0.12°C	36.42

or two times their estimated standard errors, its slope being near unity in reduced units. However, by permitting β_2 to be slightly larger than unity, the fit can be somewhat improved in most cases.

Best values for B_1 and β_1 are obtained from fits of the difference $LL_L - LL_G$ over the whole range. The values for B_1 are quite close together, from 1.92 to 1.97, but this may be accidental since B_1 is known to vary widely; thus, $B_1 = 1.43$ in He, $T_c = 5.2^\circ\text{K}$, and it is 2.15 for steam, $T_c = 647^\circ\text{K}$. The values obtained for β_1 from the fit over the whole range are 0.3450 ± 0.0006 (CO_2 , series I); 0.3475 ± 0.0006 (CO_2 , series II); 0.3482 ± 0.0007 (N_2O) and 0.354 ± 0.007 (CClF_3). However, when the range of t is somewhat reduced, the values of β_1 vary by about 0.002 so that those for CO_2 and N_2O must be considered equal. For CClF_3 the data are scarce and not very close to T_c ; a larger error in T_c is present and the value of β_1 is correlated with the choice of T_c ; thus we hesitate to conclude that this β_1 value is higher. The values of the exponents obtained here are quite close to those obtained for many other gases and reinforce the intuition that β_1 is universal.

The present data are sufficiently detailed to permit study of the asymptotic behavior. However, if older data for CO_2 and N_2O , with few points near T_c , are analyzed, the results for the asymptotic term are in quite good agreement. This shows that for the coexistence curve the asymptotic character can be ascertained in the rather large range of $|t|_{\max} = 0.09$. The difference in slope of diameter between the optical and the older data is probably due to slight density dependence of the function $(n^2 - 1)/(n^2 + 2)\rho$.

Some of the refractive index data were taken on samples with known amounts of impurity. The prime effect of impurity is a shift in T_c . The effect on B_1 is noticeable, but the exponent β_1 is virtually unchanged.

The present data, with a temperature precision of 0.001° and a precision in n of 10^{-4} , do not permit complete analysis of the term beyond the leading one in the temperature expansion of the coexisting densities. However, knowledge of this term would be suggestive in current theoretical developments. With data of the same precision, one might gain more insight in this

second term by enlarging the range of temperature. However, real progress will come only if another breakthrough in experimental precision can be achieved.

ACKNOWLEDGMENT

We have been stimulated and enlightened by numerous discussions with Dr. M. S. Green. Our cooperation was made possible by the hospitality of the Heat Division at The National Bureau of Standards, and a NATO grant to M. Vicentini-Missoni, a travel grant from the Office of Naval Research to J. Straub, and the efforts of Mr. J. Hilsenrath to arrange J. Straub's visit.

¹ J. D. van der Waals, *Z. Physik. Chem.* **13**, 657 (1894).

² J. J. van Laar, *Proc. Koninkl. Akad. Wetenschap. Amsterdam* **14**^I, 428 (1911-1912); **14**^{II}, 1091 (1911-1912).

³ R. Planck, *Forsch. Ing. Wesen* **29**, 135 (1963).

⁴ H. D. Bachr, *Forsch. Ing. Wesen* **29**, 143 (1963); *Brennstoff-Wärme-Kraft* **15**, 514 (1963).

⁵ J. E. Verschaffelt, *Comm. Leiden* **28** (1896); **55** (1900).

⁶ D. A. Goldhammer, *Z. Physik. Chem.* **71**, 577 (1910).

⁷ See, for instance, *Critical Phenomena, Proceedings of a Conference*, edited by M. S. Green and J. V. Sengers, *Natl. Bur. Std. (U.S.)*, Misc. Publ. 273 (1966).

⁸ E. H. W. Schmidt, *Ref. 7*, p. 13. J. Straub, Ph.D. thesis, München, 1965.

⁹ A. Michels, B. Blaisse, and C. Michels, *Proc. Roy. Soc. (London)* **A902**, 358 (1937).

¹⁰ D. Cook, *Trans. Faraday Soc.* **49**, 716 (1953).

¹¹ J. G. Kirkwood, *J. Chem. Phys.* **4**, 592 (1936); J. de Boer, F. van der Maesen, and C. A. Ten Seldam, *Physica* **19**, 265 (1953).

¹² A. Michels and J. Hamers, *Physica* **4**, 995 (1937). A. Michels and L. Kleerekoper, *Physica* **6**, 588 (1939).

¹³ C. P. Abbiss, C. M. Knobler, R. K. Teague, and C. J. Pings, *J. Chem. Phys.* **42**, 4145 (1965); D. E. Diller, *ibid.* **49**, 3096 (1968).

¹⁴ S. Y. Larsen, R. D. Mountain, and R. Zwanzig, *J. Chem. Phys.* **42**, 2187 (1965).

¹⁵ J. Hilsenrath, G. C. Ziegler, C. G. Messina, P. J. Walsh, and R. J. Herbold, *Ommitab, Natl. Bur. Std. (U.S.)*, Handbook **101** (1966).

¹⁶ B. Widom and J. Rowlinson, *J. Chem. Phys.* **52**, 1670 (1970); P. C. Hemmer and G. Stell, *Phys. Rev. Letters* **24**, 1284 (1970); N. D. Mermin, *Phys. Rev. Letters* **26**, 169 (1971).

¹⁷ M. S. Green, M. J. Cooper, and J. M. H. L. Sengers, *Phys. Rev. Letters* **26**, 492 (1971).

¹⁸ J. M. H. L. Sengers, *Ind. Eng. Chem. Fundamentals* **9**, 470 (1970).

¹⁹ M. E. Fisher, *Phys. Rev.* **176**, 257 (1968).

²⁰ M. E. Fisher and P. E. Scesney, *Phys. Rev. A2*, 825 (1970).